

## Spatiotemporal patterns of carbon remineralization and bio-irrigation in sediments of Casco Bay Estuary, Gulf of Maine

Mark A. Green,<sup>1</sup> Jeanne D. Gulnick, Nathaniel Dowse, and Patience Chapman

Department of Marine and Environmental Science, Saint Joseph's College of Maine, 278 Whites Bridge Road, Standish, Maine 04084

### Abstract

We measured the seasonal and spatial rates of organic matter decomposition and pore-water irrigation at four subtidal stations in Casco Bay estuary, Gulf of Maine. Organic carbon decomposition and associated flux from sediments showed strong seasonal fluctuations, with averaged highs of 44.9 ( $\pm 4.9$ ) mmol dissolved inorganic carbon (DIC)  $m^{-2} d^{-1}$  during August and lows of 8.6 ( $\pm 1.6$ ) mmol DIC  $m^{-2} d^{-1}$  during January. Apparent activation energies ( $E_{a-app}$ ) ranged from 61 ( $\pm 5.5$ ) to 83 ( $\pm 14.5$ ) kJ  $mol^{-1}$  in the 0–1 and 2–3 cm layers of sediments, respectively, which reflects a decrease in carbon reactivity with depth. Spatial differences in surface  $E_{a-app}$  correlate with C:N ratios in pore water, with lowest  $E_{a-app}$  levels at stations with lowest C:N; ratios, which is consistent with the remineralization of recently formed organic matter. In addition, there was a significant time-dependent change in the transport mechanism between sediments and overlying water. Br<sup>-</sup> tracer experiments, comparison of flux estimates, and diagenetic transport-reaction models all independently showed that transport increases significantly because of the activities of benthos during spring, summer, and fall, when rates are ~3 times higher than simple diffusion alone. Biologically enhanced transport resulted from the high density of benthos (>1.0 mm, ~7,000  $m^{-2}$ ), with the nephtyid polychaete *Aglaophamus neotenus* and the spionid polychaete *Prionospio steenstrupi* being most abundant. The polychaete *Owenia fusiformis* and the burrowing, deposit-feeding amphipod *Casco bigelowi* were also important. These results further confirm the importance of understanding seasonal variability in both carbon degradation and the influence of benthic organisms in controlling material exchange between sediments and water in estuarine systems.

The organic matter produced in the coastal ocean and deposited to underlying sediments provides a reductant for microbial metabolic activity and causes the release of biologically important metabolites such as dissolved inorganic carbon (DIC), NH<sub>4</sub><sup>+</sup>, Si, and HPO<sub>4</sub><sup>3-</sup>, as well as the consumption of O<sub>2</sub> and other terminal electron acceptors (e.g., Froelich et al. 1979). The release and consumption of these solutes depends on the coupled interaction between degradation rates and transport across the sediment-water interface (SWI; Berner 1980), and both must be understood to quantitatively describe solute flux and the coupling between nutrient release and biological uptake in nearshore environments. Resolving seasonal and spatial patterns of carbon degradation and solute transport is important, yet particularly difficult, in temperate estuaries where large changes in temperature, carbon flux, and benthic community activity occur over rapid timescales and/or across short horizontal distances (e.g., Middelburg et al. 1996).

It is well documented that marine benthic organisms can significantly enhance the transport of solutes and particles between sediments and overlying water to rates well above

those of simple molecular diffusion and sedimentation (Aller 1978; Boudreau 1986; Green et al. 2002; Meile and Van Cappellen 2003). Biologically enhanced transport of particles and solutes at the SWI controls the pathways and rates of C decomposition, influences the mass flux of important nutrients, and ultimately affects the storage of residual carbon in marine sediments. Recent estimates have suggested that, globally, “biologically enhanced” transport between sediments and overlying water could contribute upward of 33% and 50% of the total benthic O<sub>2</sub> and PO<sub>4</sub><sup>3-</sup> flux, respectively (Meile and Van Cappellen 2003). Jahnke (2001) reported a correlation between total O<sub>2</sub> uptake by sediments and the relative importance of enhanced solute transport where regions with higher total O<sub>2</sub> flux have a greater proportion of flux attributed to biologically enhanced mechanisms (e.g., biodiffusion and bio-irrigation). That is, flux across the SWI in coastal deposits is more likely to be biologically accelerated above diffusive rates compared with flux in the deep sea.

The primary purpose of the present study was to document seasonal and spatial patterns of carbon remineralization and solute transport mechanism (diffusion vs. bio-enhanced) in Casco Bay Estuary, a well-mixed estuary located along the central southern Maine coast. Although many studies of benthic remineralization of organic matter in estuaries exist, very few have considered both spatial and temporal changes in the remineralization rate and the effect of benthos on material transport rate across the SWI. Although Casco Bay deposits have been studied in the past, research to date has focused exclusively on the distribution of organic contaminants and metals in surface sediments (Larsen et al. 1983; Kennicutt et al. 1994; Wade et al. 1995; Wenning et al. 1998;

<sup>1</sup> Corresponding author (mgreen@sjcme.edu).

### Acknowledgments

This research greatly benefited from the hard work and dedication of Chris Renaud, Nickie Charrette, Kelly Beaudoin, Joseph Glowa, and Carrie Boudreau. We thank the captain and crew of the R/V 7 for their hospitality on the high seas. Our manuscript was improved through the insight and comments of J. Middelburg and two anonymous reviewers.

This research was supported by National Science Foundation CA-REER grant OCE-9984708 to M.A.G.

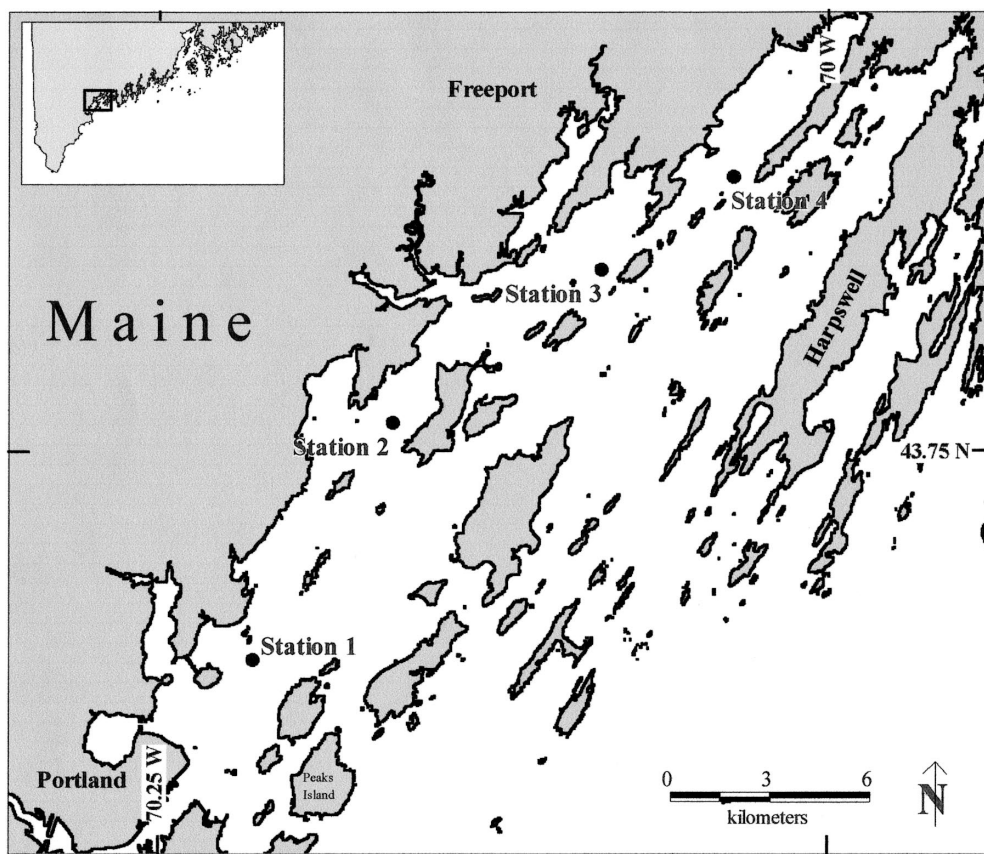


Fig. 1. Map of Casco Bay Estuary showing the four study stations

Golomb et al. 2001). There have been no published studies to date on the early diagenetic processes near the SWI in Casco Bay Estuary, despite the estuary's designation as a national treasure and its inclusion in the National Estuary Program (Casco Bay Estuary Project 1996).

#### Materials and methods

*Study location and sampling protocol*—Casco Bay is a well-mixed estuary located along the south-central Maine coast and is characterized as a northern temperate/southern boreal climate with a large tidal range (3 m). Sampling was conducted at four stations in Casco Bay estuary (Fig. 1) as part of the Carbonate Solubility in the Coastal Ocean study from November 2000 through December 2001 and followed the same sampling protocol for each of the 11 cruises. A GOMEX-2525 box corer (625 cm<sup>2</sup>) was used to collect bottom sediment and overlying water during each cruise from which butyrate subcores (9.5 cm inner diameter) were removed. The GOMEX box corer yielded well-defined, undisturbed sediments, as was evident from clear water above the SWI. All cores were stored at in situ temperature prior to processing back at the laboratory (within 8 h). In general, water depth at all stations ranged 6–8 m, sediments were muddy, consisted of ~3–5% organic carbon (~10% loss on ignition, LOI) and 1–3 wt. % CaCO<sub>3</sub> and had an average surface sediment (0–1cm) porosity ( $\phi$ ) of ~0.9. Salinities

varied slightly throughout the year and/or from station to station and ranged 30–33. Cruise numbers, sampling dates, corresponding day of the year, surface and bottom water temperatures, and surface water chlorophyll *a* during each cruise are given in Table 1.

*Sediment incubation and production flux of DIC*—Short-term sediment incubation experiments (72 h) were used to measure net rates of DIC production from 0–1, 1–2, and 2–3 cm in cores collected from each station. Depth-dependent rates of DIC production were used to estimate DIC “production” flux throughout the year. Two cores (9.5 cm inner diameter) were removed from the box-corer at each station and stored at in situ temperature for transport back to the lab. Both cores were sectioned under N<sub>2</sub> in a glove bag at 0–1, 1–2, and 2–3 cm before sediment from each depth was pooled in a glass beaker and homogenized by gentle stirring. All macroscopic benthic fauna were picked out of sediments using forceps. Mixed sediment from each interval was used to fill four 25-ml plastic scintillation vials. Vials were incubated under O<sub>2</sub> free conditions by placing in anoxic sediments at in situ temperature and sampling daily for 3 d. At each time point, pore waters were separated using centrifugation (N<sub>2</sub> environment, in situ temperature, 10–15 min, 2236 g), filtered through a 0.45- $\mu$ m Acrodisc filter, and a 1-ml sample used to measure DIC by flow injection analysis and conductivity detection (Hall and Aller 1992).

Table 1. Cruise number, cruise date, corresponding day of the year, surface (SW) and bottom (BW) water temperatures, and surface water Chl *a*.

Cruise no.	Month	Date	Day of the year	SW temp (°C)	BW temp (°C)	Average SW Chl <i>a</i> ( $\mu\text{g L}^{-1}$ )
C-2	November	16 Nov 00	-45	8.8	9.5	2.2±0.9
C-3	January	03 Jan 01	3	2.0	2.4	2.9±1.2
C-4	February	05 Feb 01	35	1.7	1.7	8.7±2.2
C-5	March	04 Mar 01	63	0.6	0.4	2.2±0.7
C-6	April	16 Apr 01	100	6.3	5.1	1.2±0.1
C-7	May	08 May 01	122	10.6	8.6	1.6±0.8
C-8	June	19 Jun 01	164	18.7	11.8	2.3±0.3
C-9	July	24 Jul 01	199	17	15.0	2.2±1.0
C-10	August	27 Aug 01	233	16.7	16.1	2.6±0.8
C-11	October	14 Oct 01	281	13.4	13.0	3.3±2.0
C-12	December	10 Dec 01	338	6.4	7.6	1.9±0.4

O<sub>2</sub> penetration into sediments ranged from ~1 mm during summer to ~4 mm during winter at all four stations, which indicates that, in the 0–1 cm depth interval of incubated sediment, some of the seasonal changes in DIC production may have come from differences in initial O<sub>2</sub> availability (i.e., the metabolic pathway). However, these O<sub>2</sub> penetration depths, maximum SWI O<sub>2</sub> concentrations of ~300  $\mu\text{mol L}^{-1}$ , and the measured DIC production rates all suggest that trapped O<sub>2</sub> should have been consumed far more rapidly (minutes) compared with the daily intervals between sampling points. Plots of DIC production over the 3-d incubation period showed perfect to near-perfect linearity ( $r^2 > 0.9$ ) during each incubation series, which suggests that free O<sub>2</sub> in the 0–1 cm incubations was quickly consumed and that DIC production came from metabolic pathways that were almost exclusively anaerobic in nature.

*Diffusive flux from pore-water gradients*—Fick's first law of diffusion (Berner 1980) was used to calculate flux of DIC from sediment pore-water profiles during each cruise. One core from each station (9.5 cm inner diameter) was sectioned under N<sub>2</sub> in a glove bag (0–0.5, 0.5–1.0, 1.0–2.0, 2.0–3.0, 3.0–4.0, 4.0–5.0, 5.0–7.0, and 7.0–10.0 cm), pore water was separated, and DIC was measured as described previously.

Gradients ( $dC/dz$ ) from the near-linear portion of the pore water profile (3–4 points) were used to calculate flux ( $J$ ) for DIC according to

$$J = -\phi_0 D_s (dC/dz) \quad (1)$$

where  $\phi_0$  is the porosity at  $z = 0$  cm,  $D_s$  is the whole-sediment diffusion coefficient for, in this case, HCO<sub>3</sub><sup>-</sup>, and  $dC/dz$  is the linear portion of the solute concentration gradient. The use of  $D_s$  for HCO<sub>3</sub><sup>-</sup> is reasonable, given the pH range of sediment (~6.8–7.4) measured. Porosity was determined from the water content using the equation

$$\phi = \omega^* \rho_s / (\omega^* \rho_s + (1 - \omega) \rho_w) \quad (2)$$

where  $\omega$  is the weight fraction of H<sub>2</sub>O,  $\rho_s$  is the sediment density assumed to be 2.65 g solid cc-sediment<sup>-1</sup>, and  $\rho_w$  is the water density, assumed to be 1.02 g cm<sup>-3</sup> H<sub>2</sub>O<sup>-1</sup>.

*Br<sup>-</sup> tracer experiments for estimates of transport rate*—Time-series changes in concentrations of Br<sup>-</sup> added to intact

sediment cores were used to evaluate the mass flux of Br<sup>-</sup> into sediments and the solute transport rate during each cruise at all stations (Martin and Banta 1992; Green et al. 2002). Br<sup>-</sup> is a conservative tracer in surface pore water of marine deposits, at least over the short timescales of the incubations used in this study (24–48 h; Mackin et al. 1989).

One subcore containing overlying water was fitted with o-ring-sealed caps, aerated, and gently stirred with small stirring motors at in situ temperature. Overlying water was spiked with ~0.5 g KBr (first dissolved in ~5 ml of bottom water removed directly from the core), and aliquots were analyzed for Br<sup>-</sup> 4–5 times for 24–48 h, using the method of Presley (1971). Br<sup>-</sup> concentrations as a function of time in overlying water were compared with theoretical estimates of Br<sup>-</sup> redistribution in a finite volume of water overlying sediment, as predicted from a one-dimensional, diffusive transport model that assumed no reaction (an explicit finite-difference scheme checked with an exact analytical solution). The Br<sup>-</sup> loss from overlying water was quantified using a constant transport coefficient that best-fit measured Br<sup>-</sup> concentrations with model estimates (Green et al. 2002).

In addition to model-predicted estimates of transport rate, the molecular diffusion transport ( $D_s$ ) was also calculated for Br<sup>-</sup> using sediment porosity from each station during each cruise according to Berner (1980):

$$D_s^{\text{Br}} = \phi^2 D_o^{\text{Br}} \quad (3)$$

where  $\phi$  is the porosity at  $z = 0$  cm and  $D_o^{\text{Br}}$  is the free solution diffusion coefficient for Br<sup>-</sup>, corrected for in situ temperature and viscosity using the Stokes Einstein relation (Li and Gregory 1974).

For the present study, we assumed that model estimates of transport greater than those based on simple molecular diffusion (Eq. 3) resulted from increases in solute transport at the SWI by activities of benthic organisms. In this case, a quasi diffusive or apparent-diffusive term ( $D_{\text{app}}$ ) sufficient to account for measured Br<sup>-</sup> transport was used to describe solute mobility across the SWI. The use of a  $D_{\text{app}}$  coefficient often provides a reasonable estimate of transport mode, because competing infaunal, epifaunal, and molecular transport processes can mimic random eddy diffusivity because of the variety of transport processes within a given area. Other investigators, in both freshwater and marine systems, have

Table 2. Compilation of DIC reaction-rate data from sediment incubations for each cruise and at each study station.

Cruise no.	Month	Sta. 1			Sta. 2			Sta. 3			Sta. 4			Avg $J_{\text{DIC}}$ ( $\pm$ SD) (mmol $\text{m}^{-2} \text{d}^{-1}$ )
		$R_o$	$\alpha$	$J_{\text{DIC}}$	$R_o$	$\alpha$	$J_{\text{DIC}}$	$R_o$	$\alpha$	$J_{\text{DIC}}$	$R_o$	$\alpha$	$J_{\text{DIC}}$	
C-2	Nov	1.20	0.90	12.4	1.04	0.55	17.1	1.04	0.55	17.33	1.11	0.61	16.5	15.85 $\pm$ 2.32
C-3	Jan	0.59	0.85	6.45	0.63	0.61	9.38	0.49	0.46	10.15	0.61	0.64	8.34	8.55 $\pm$ 1.46
C-4	Feb	0.81	0.80	9.46	0.65	0.53	11.73	0.42	0.47	8.13	0.57	0.79	6.62	8.98 $\pm$ 2.17
C-5	Mar	0.85	0.69	11.44	0.76	0.56	12.31	0.94	0.78	11.11	0.64	0.32	17.40	13.07 $\pm$ 2.93
C-6	Apr	1.52	0.88	16.1	1.30	0.72	16.4	0.46	0.22	17.0	0.74	0.61	11.01	15.13 $\pm$ 2.77
C-7	May	3.03	1.21	23.3	2.08	0.60	31.47	1.17	0.24	40.78	1.02	0.73	12.71	27.06 $\pm$ 11.94
C-8	Jun	3.53	0.80	41.07	2.29	0.58	36.06	1.40	0.33	37.2	3.20	0.96	30.43	36.19 $\pm$ 4.40
C-9	Jul	2.41	0.43	51.42	1.80	0.34	46.57	1.88	0.51	33.64	1.88	0.51	25.4	39.26 $\pm$ 11.9
C-10	Aug	2.83	0.52	50.33	3.20	0.69	38.73	1.60	0.30	46.62	2.05	0.42	43.75	44.86 $\pm$ 4.89
C-11	Oct	1.63	0.61	24.76	1.88	0.83	20.61	0.78	0.46	15.44	1.70	0.74	20.9	20.42 $\pm$ 3.82
C-12	Dec	1.93	0.93	19.30	1.52	0.51	26.96	0.91	0.60	13.9	1.46	0.37	35.02	23.80 $\pm$ 9.20

$R_o$ : DIC production at the sediment water interface ( $\mu\text{mol DIC cm}^{-3} \text{ sed d}^{-1}$ ),  $\alpha$  reaction-rate attenuation. Also shown are the production flux estimates, generated using reaction-rate data and Eqs. 4 and 5. The station-averaged production flux (mmol DIC  $\text{m}^{-2} \text{d}^{-1}$ ) is also given for each cruise.

found that lumping the effects of biogenic reworking into an apparent diffusion coefficient can adequately constrain transport in some cases (Goldhaber et al. 1977; Vanderborght et al. 1977; Fisher 1982; Green and Aller 1998, 2001). As is

discussed below, this may be particularly true in Casco Bay, where both benthic density and diversity are extremely high (Larsen et al. 1980). In addition, this model tends to be a good approximation of transport rate when the biological reworking is limited to the near-surface sediments of the deposit, the length scale of transport is relatively small, and the transport time is short (e.g., hours to days).

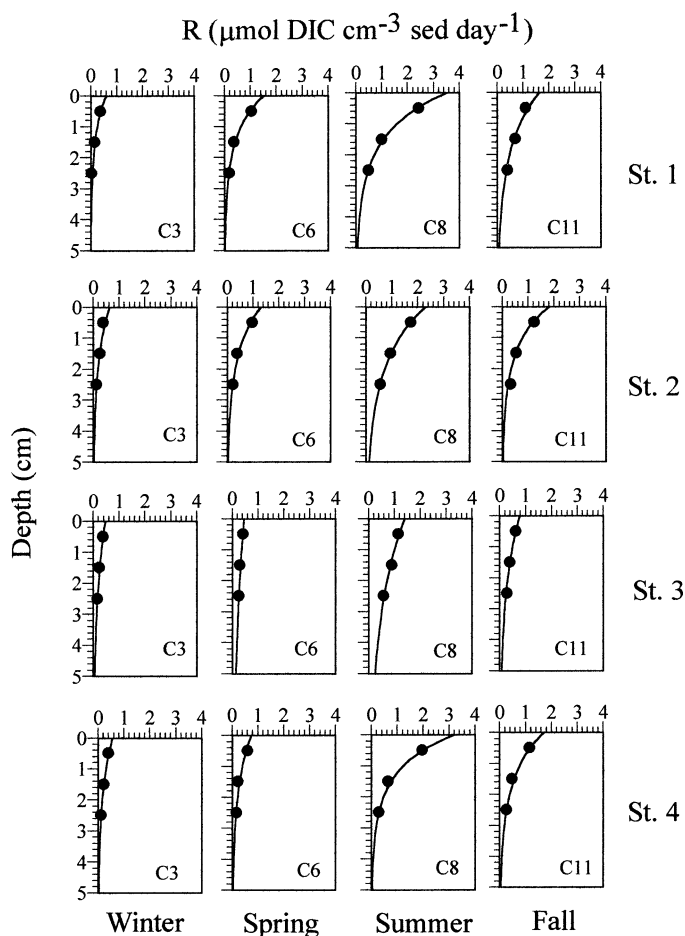


Fig. 2. Measured (circles) and modeled (solid line) DIC reaction rate ( $\mu\text{mol cm}^{-3} \text{ sed day}^{-1}$ ) in sediments during representative seasonal cruises at each of the study stations. DIC reaction-rate data from all cruises and stations can be found in Table 2.

*Additional measurements*—Surface-water samples were collected during each cruise using a Niskin Bottle, and 180 ml was filtered through Whatman GFF filters. Chl *a* was extracted for 24 h in a freezer in the dark using 90% acetone (v/v) and measured using a Turner Design TD-700 fluorometer. Macrofauna were collected using an Eckman Grab at each station during the August cruise (C10). Sediment was sieved through a 1-mm sieve, stored in 4% buffered formalin, and stained with Rose Bengal prior to identification.  $\text{NH}_4^+$  was measured in pore water from sediment intervals sectioned for DIC analysis according to the method of Solozano (1969).

## Results

*Sediment incubations and DIC production flux*—Production rates for DIC during anoxic incubation experiments were calculated as the slope of the DIC concentration versus incubation time and converted to units of mass/sediment volume/time using measured porosities from each depth interval (0–1, 1–2, and 2–3 cm).

During each cruise, DIC production decreased exponentially with depth in the deposit so that the reaction rate,  $R$ , at any depth,  $z$ , could be evaluated using the commonly accepted rate form

$$R_z = R_o \exp^{-\alpha z} \quad (4)$$

where the natural log transformation of DIC production rates ( $\mu\text{mol DIC cc sediment}^{-1} \text{d}^{-1}$ ) versus depth provided an intercept equal to DIC production at  $z = 0$  cm ( $R_o$ ) and a slope equivalent to reaction attenuation ( $\alpha$ ). Values for  $R_o$  and  $\alpha$  are provided in Table 2.

Figure 2 shows DIC reaction rate versus depth at each

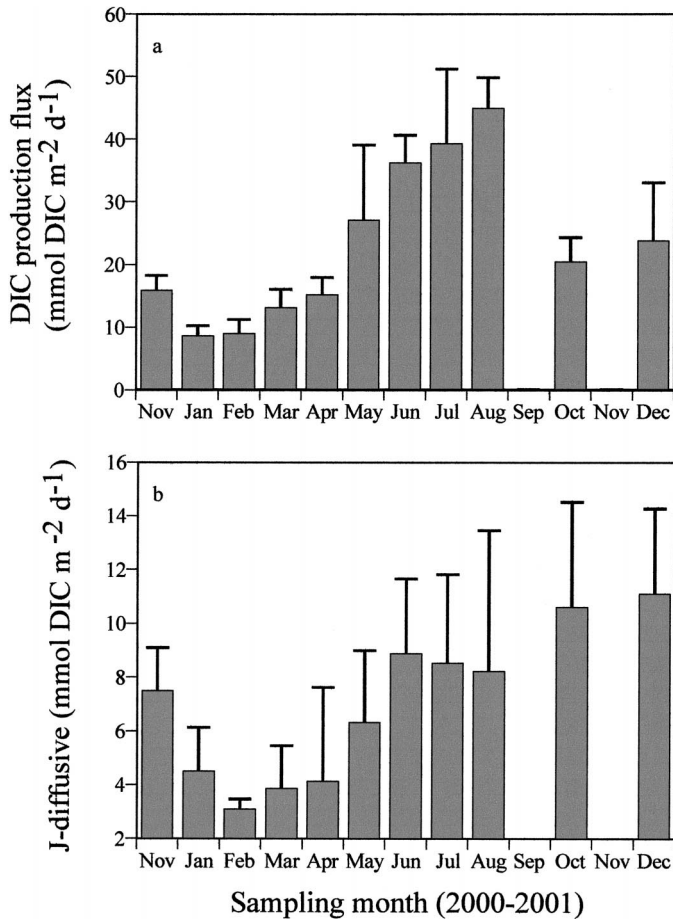


Fig. 3. Station-averaged seasonal DIC flux. (a) Production flux of DIC, estimated using sediment incubations. (b) Diffusive estimates of DIC, flux estimated using pore-water DIC gradients and the molecular diffusion coefficient  $D_s$  for  $\text{HCO}_3^-$ . Units are  $\text{mmol DIC m}^{-2} \text{d}^{-1} \pm \text{SD}$ .

station during winter (January; C3), spring (April; C6), summer (June; C8), and fall (October; C11), using both measured (0–1, 1–2, and 2–3 cm) and modeled (Eq. 4) values. Modeled estimates accurately predicted measured values with depth in each core. Although not shown, modeled estimates of DIC reaction rate closely approximated measured values from all other cruises. At each station, the DIC production rate at the SWI was 2–4 times higher during summer than during winter. DIC production fluxes were calculated by taking the integral of the depth-dependent production rate (Eq. 4) from 0–10 cm,

$$J_{\text{production}} - \text{DIC} = \int_0^{10} R_o \exp^{-\alpha z} \quad (5)$$

and are shown in Table 2. Although some spatial heterogeneity exists, station-averaged DIC flux for each cruise (Table 2, Fig. 3a) showed SDs that were typically only ~10–30% of the mean. There was no observable regular pattern in which one or more stations had DIC production flux that remained consistently higher or lower than others over the course of the year. There were, however, considerable sea-

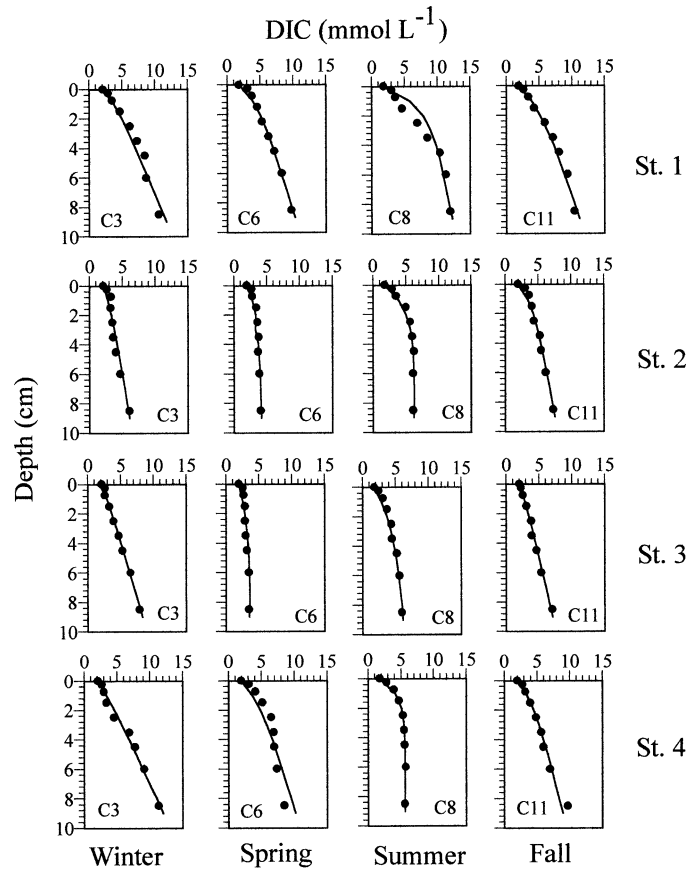


Fig. 4. Measured (circles) and modeled (solid line) pore-water DIC concentrations ( $\text{mmol L}^{-1}$ ) during representative seasonal cruises at each of the study stations.

sonal differences in DIC production throughout the estuary, where the flux during summer (June–August) was generally 4–5 times that of measurements obtained during winter (January–March). Station-averaged DIC fluxes ranged from a low of  $8.55 \pm 1.46$  during January to a high of  $44.86 \pm 4.89$   $\text{mmol DIC m}^{-2} \text{d}^{-1}$  during August (Table 2, Fig. 3a). Sediments at all stations were undersaturated with respect to calcite and aragonite predominantly during summer cruises, so the dissolution of  $\text{CaCO}_3$  might have increased the apparent production of DIC from carbon remineralization in sediment incubations. However, in the absence of diffusive loss, the high measured DIC production during warmer months should have rapidly shifted carbonate saturation states to supersaturated conditions in the closed sediment incubations, which suggests that  $\text{CaCO}_3$ -contributed DIC was likely negligible. However, this is only a supposition, because saturation states were never measured in incubated sediments.

*Diffusive flux based on pore-water gradients*—Dissolved DIC in pore water is shown for Sta. 1–4 during representative cruises for winter (C3), spring (C6), summer (C8), and fall (C11) in Fig. 4. DIC concentrations during these and all other cruises (not shown) increased from bottom-water values ~2.1  $\text{mmol L}^{-1}$ , and, in most cases, approached concentrations of 5–8  $\text{mmol L}^{-1}$  by 8 cm. Diffusive fluxes of

Table 3. Compilation of pore-water DIC data.

Cruise no.	Month	Sta. 1			Sta. 2			Sta. 3			Sta. 4			Avg $J_{\text{DIC}}$ ( $\pm$ SD) (mmol m <sup>-2</sup> d <sup>-1</sup> )
		$\partial C/\partial x$	$D_s$	$J_{\text{DIC}}$	$\partial C/\partial x$	$D_s$	$J_{\text{DIC}}$	$\partial C/\partial x$	$D_s$	$J_{\text{DIC}}$	$\partial C/\partial x$	$D_s$	$J_{\text{DIC}}$	
C-2	Nov	1.03	0.73	6.88	1.21	0.73	8.07	0.84	0.73	5.63	1.40	0.73	9.34	7.48 $\pm$ 1.59
C-3	Jan	1.34	0.56	6.84	0.65	0.56	3.34	0.69	0.56	3.54	0.84	0.56	4.28	4.50 $\pm$ 1.61
C-4	Feb	*	*	*	0.53	0.56	2.74	0.61	0.56	3.13	0.67	0.56	3.44	3.10 $\pm$ 0.35
C-5	Mar	0.82	0.52	3.91	0.34	0.52	1.62	0.98	0.52	4.68	2.09	0.52	5.20	3.85 $\pm$ 1.58
C-6	Apr	0.93	0.62	5.28	0.36	0.62	2.04	0.24	0.62	0.72	1.49	0.62	8.46	4.13 $\pm$ 3.47
C-7	May	1.45	0.70	9.38	*	*	*	0.54	0.70	4.71	0.75	0.70	4.84	6.31 $\pm$ 2.66
C-8	Jun	1.78	0.77	12.62	1.70	0.77	9.10	0.86	0.77	6.10	1.50	0.77	7.66	8.87 $\pm$ 2.78
C-9	Jul	0.90	0.84	6.97	0.61	0.84	4.76	1.31	0.84	10.15	1.57	0.84	12.16	8.51 $\pm$ 3.29
C-10	Aug	0.97	0.87	7.75	0.72	0.87	5.75	0.46	0.87	3.68	1.96	0.87	15.64	8.21 $\pm$ 5.23
C-11	Oct	0.83	0.79	6.07	2.03	0.79	14.83	1.73	0.79	12.64	1.21	0.79	8.84	10.60 $\pm$ 3.90
C-12	Dec	1.06	0.68	6.64	2.21	0.68	13.84	1.78	0.68	11.15	2.03	0.68	12.71	11.09 $\pm$ 3.16

$\partial C/\partial x$ : linear portion of the DIC pore-water gradient (mmol cm<sup>-3</sup> cm<sup>-1</sup>),  $D_s$ : estimated diffusion coefficient for HCO<sub>3</sub><sup>-</sup>, calculated from sediment using the free solution diffusion coefficient for HCO<sub>3</sub><sup>-</sup> and corrected for in situ temperature and viscosity using the Stokes Einstein relations (Li and Gregory 1974) and porosity (Eq. 2). Also shown is the gradient-predicted flux from each station and the station-averaged flux from each cruise (mmol m<sup>-2</sup> d<sup>-1</sup>).

\* Data not available.

DIC were calculated using the near-linear portion of the pore-water gradient (usually the surficial 3–4 points) and Eq. 1. Pore-water gradients, molecular diffusion coefficients, and station-specific and -averaged DIC flux for each cruise are provided in Table 3.

Averaged DIC fluxes from pore-water gradients are shown in Fig. 3b and ranged from a low during February of 3.1  $\pm$  0.35 to a high during December of 11.09  $\pm$  3.16 mmol m<sup>-2</sup> d<sup>-1</sup>. Although the seasonal pattern of change of the gradient estimated flux resembled those from sediment incubations, fluxes from pore-water gradients were considerably less at any given station during each cruise than those based on incubated sediments (Table 2, Fig. 3a). In addition, the gradient-predicted flux showed far greater station-to-station differences on any given cruise, with SDs of station-averaged flux typically >40% of the mean. As discussed below, spa-

tial differences in gradient flux estimates likely resulted from different rates of bio-irrigation, which will alter a gradient's geometry by dilution with overlying water. This will cause an underestimate of gradient-predicted flux because transport will be greater than molecular diffusion ( $D_s$ ) when and where bio-irrigation is occurring and the concentration gradient has been lowered.

*Br<sup>-</sup> tracer experiments*—An example of a model fit to Br<sup>-</sup> loss in water overlying flux cores and a comparison with diffusive predicted Br<sup>-</sup> loss is given in Fig. 5. Rates of solute transport estimated from Br<sup>-</sup> incubations ( $D_{\text{app}}^{\text{Br}}$ ), along with molecular-diffusion coefficients for Br<sup>-</sup> ( $D_s^{\text{Br}}$ ) calculated from Eq. 3, are provided in Table 4. In general, values of  $D_{\text{app}}^{\text{Br}}$  were higher than diffusive coefficients during spring, summer, and early fall, with the largest discrepancy during summer, when transport was 2–3 times that of simple molecular diffusion. This time-dependent change in transport is shown in Fig. 6a, where the station-averaged  $D_{\text{app}}^{\text{Br}}:D_s^{\text{Br}}$  ratio during each cruise provides clear evidence of a seasonal change in transport regime, with biologically enhanced transport dominating material flux across the SWI during all seasons except late fall and winter.

## Discussion

When a marine deposit is in steady state with respect to reaction and transport, the sum of all reactions within the deposit should balance the flux of products across the SWI. With the assumption of “local” steady state, the seasonal and spatial patterns of DIC flux in Casco Bay were estimated through the integration of measured DIC production from discrete sediment intervals (Table 2, Fig. 3a). Despite Casco Bay's northern temperate/southern boreal climate, average estimates of DIC production flux range annually from ~8 to 25 mmol m<sup>-2</sup> d<sup>-1</sup> during winter and 25 to 45 mmol m<sup>-2</sup> d<sup>-1</sup> during summer and are in a similar range or higher than flux estimates generated using the same technique from more southern estuaries. For example, Mackin and Swider (1989) used sediment incubations to calculate the DIC flux from

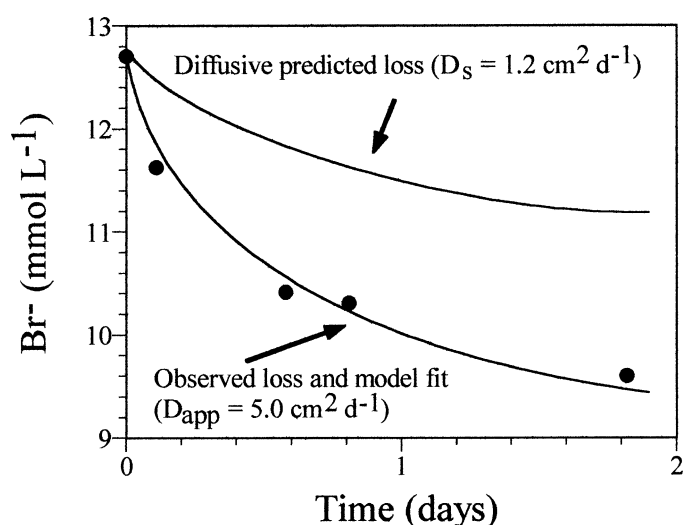


Fig. 5. Example of a typical model fit to the loss of measured Br<sup>-</sup> concentrations (circles) in water overlying Br<sup>-</sup> spiked flux cores. An example of the modeled loss of Br<sup>-</sup> under the assumption of transport of Br<sup>-</sup> into sediments by simple molecular diffusion is also given. Units of  $D_s$  are cm<sup>2</sup> d<sup>-1</sup>.

Table 4. Estimates of “apparent” transport of  $\text{Br}^-$  across the sediment-water interface from each station at each cruise ( $D_{\text{app}}$ ,  $\text{cm}^2 \text{d}^{-1}$ ). The transport rate was calculated using a  $\text{Br}^-$  tracer and model fits to  $\text{Br}^-$  loss in water overlying spiked cores. Also shown are estimates of the diffusive transport of  $\text{Br}^-$  ( $D_s$ ) and the  $D_{\text{app}}:D_s$  ratio.

Cruise no.	Month	Sta. 1	Sta. 2	Sta. 3	Sta. 4	Average $D_{\text{app}}$	$D_s \text{ Br}^-$	Avg $D_{\text{app}}:D_s$
C-2	Nov	1.0	1.0	1.1	—	$1.0 \pm 0.1$	1.0	$1.0 \pm 0.1$
C-3	Jan	—	1.0	0.8	0.8	$0.9 \pm 0.1$	0.8	$1.1 \pm 0.1$
C-4	Feb	1.0	1.0	0.8	1.0	$1.0 \pm 0.1$	0.78	$1.2 \pm 0.1$
C-5	Mar	0.8	1.4	3.0	3.0	$2.1 \pm 1.1$	0.75	$2.6 \pm 1.4$
C-6	Apr	0.9	4.0	3.0	3.3	$2.8 \pm 1.3$	0.88	$3.2 \pm 1.5$
C-7	May	3.1	2.3	1.8	5.0	$3.1 \pm 1.4$	0.98	$3.1 \pm 1.4$
C-8	Jun	1.8	2.5	2.5	—	$2.3 \pm 0.4$	1.07	$2.1 \pm 0.4$
C-9	Jul	2.5	2.0	—	2.5	$2.3 \pm 0.3$	1.15	$2.0 \pm 0.3$
C-10	Aug	5.0	6.0	3.0	1.8	$4.0 \pm 1.9$	1.19	$3.3 \pm 1.6$
C-11	Oct	1.1	—	2.2	2.5	$1.9 \pm 0.7$	1.1	$1.8 \pm 0.7$
C-12	Dec	0.9	0.9	1.5	0.9	$1.1 \pm 0.3$	0.95	$1.1 \pm 0.3$

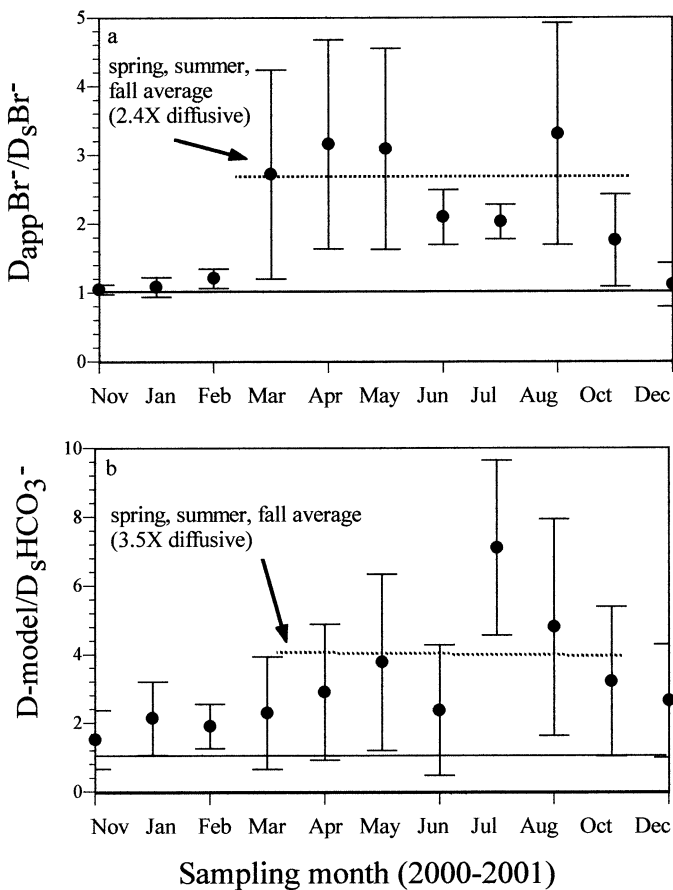


Fig. 6. Ratio of estimates of transport to that of molecular diffusion. (a) Ratio of the measured transport rate of  $\text{Br}^-$  ( $D_{\text{app}}$ ), calculated using the  $\text{Br}^-$  tracer to estimates of transport, under the assumption of simple molecular diffusion ( $D_s$ ). Individual values represent averages from the four study stations ( $\pm \text{SD}$ ) during each cruise. Transport is accelerated, on average, 2.4 times above simple molecular diffusion during spring, summer, and fall seasons. (b) Ratio of modeled transport rate of DIC ( $D\text{-model}$ ) to estimates of DIC transport, under the assumption of simple molecular diffusion ( $D_s - \text{HCO}_3^-$ ). Individual values represent averages from the four study stations ( $\pm \text{SD}$ ) during each cruise. Transport was accelerated, on average, 3.5 times above simple molecular diffusion during spring, summer, and fall.

Sta. 9 in western Long Island Sound equivalent to 17 and 33  $\text{mmol DIC m}^{-2} \text{d}^{-1}$  in January and August, respectively. Green (1998) reported DIC flux from the more eastern Sta. P in Long Island Sound ranging from  $\sim 2$  to 20  $\text{mmol m}^{-2} \text{d}^{-1}$  during winter and summer, respectively. High DIC production in Casco Bay relative to more southern estuaries is indicative of the generally high reactivity of sediments in this region.

The average production flux of DIC in Casco Bay sediments translates to annual C-organic oxidation rates of 114, 110, 95, and 89  $\text{g C m}^{-2}$  at Sta. 1–4 and compares well with rates reported for other coastal deposits. For example, annual rates of organic matter remineralization in Westerschelde Estuary range from 96 to  $\sim 4,000 \text{ g C m}^{-2} \text{yr}^{-1}$  (Middelburg et al. 1996). McNichol et al. (1988) reported an annual average of 69  $\text{g C m}^{-2} \text{yr}^{-1}$  oxidized in surface sediments of Sta. M in Buzzards Bay, and Henrichs and Farrington (1987) calculated that 14  $\text{g C m}^{-2}$  are oxidized annually in surface sediments of Sta. P in Buzzards Bay. Multiple studies in Cape Lookout Bight, North Carolina, have provided a range of C oxidation from  $\sim 30$  to  $\sim 500 \text{ g C m}^{-2} \text{yr}^{-1}$  (Martens and Klump 1984; Chanton et al. 1987; Crill and Martens 1987; Martens et al. 1992).

*Temperature dependence on carbon decomposition*—Numerous studies have demonstrated the dependence of the diagenetic reaction rate on temperature (Middelburg et al. 1996). In the present study, bottom-water temperatures ranged 0.4–16.1°C over the course of the year, and this is one reason for the distinct seasonality of DIC production (Fig. 3a, Table 2). DIC production rate data from 0–1, 1–2, and 2–3 cm were fitted to the Arrhenius equation, to determine the temperature dependence on DIC flux in Casco Bay:

$$\text{DIC production rate} = Ae^{-E_a/RT} \quad (6)$$

where  $A$  is the preexponential factor,  $E_a$  is the activation energy ( $\text{kJ mol}^{-1}$ ),  $T$  is the absolute temperature, and  $R$  is the gas constant, which in this case is equivalent to 8.314  $\text{J mol}^{-1} \text{deg}^{-1}$ . The slopes of the natural log of production rates from the 0–1, 1–2, and 2–3 cm incubations versus the reciprocal of absolute temperature gave a straight line with a slope equal to  $-E_a/R$ . Thus,  $E_a$  can be determined for sediments at each station in Casco Bay. In this case, how-

Table 5. Apparent activation energies ( $E_{a-app}$  kJ mol<sup>-1</sup>) for sediments from 0–1, 1–2, and 2–3-cm intervals from each study station. Also shown are the station-averaged  $E_{a-app}$  values for each sediment depth.

Depth (cm)	Sta. 1	Sta. 2	Sta. 3	Sta. 4	Average $E_{a-app}$
0–1	67	57	55	63	61 ± 5.5
1–2	70	62	50	49	58 ± 10.1
2–3	100	68	74	89	83 ± 14.5

ever,  $E_a$  should be considered the “apparent” activation energy,  $E_{a-app}$ , which is more appropriately considered as a total “biogeochemical” (e.g., microbial community, substrate composition, and substrate variability) response of carbon remineralization to temperature change (Westrich and Berner 1988).

Table 5 shows  $E_{a-app}$  for the 0–1, 1–2, and 2–3 cm depth intervals for each of the four study locations. In the absence of any down-core variability in temperature and carbon reactivity/microbial activity,  $E_{a-app}$  values from 0–1, 1–2, and 2–3 cm should be equal at any given station. At all stations, there were uniform temperatures in sediments measured through the top 5 cm; however, apparent activation energies were consistently lower in surface sediments compared with the 2–3 cm depth interval, with Sta. 1 and 2 showing a steady increase in  $E_{a-app}$  from 0 to 3 cm. The down-core increase in  $E_{a-app}$ , despite no temperature gradient, is consistent with a decrease in carbon reactivity with depth (Westrich and Berner 1988; Middelburg et al. 1996).

Apparent activation energies for carbon remineralization in Casco Bay (50–100 kJ mol<sup>-1</sup>) are similar to the range of those reported in the literature from other estuaries. Early work by Vosjan (1974) calculated apparent activation energies for Wadden Sea sediments of 92 kJ mol<sup>-1</sup>. Goldhaber et al. (1977) gave  $E_{a-app}$  of ~105 kJ mol<sup>-1</sup> at the FOAM site in Long Island Sound. Mackin and Swider (1989) used sediment incubations to calculate  $E_{a-app}$  in Flax Pond, a tidal marsh in Long Island Sound, of 75 and 88 kJ mol<sup>-1</sup> in the 0–3 and 3–6 cm intervals of sediment, respectively. Middelburg et al. (1996) reported a range of apparent activation energies of 54–125 kJ mol<sup>-1</sup> along an eight-station gradient in the Westerschelde Estuary, with only the extreme upper estuary stations of Durme and Notelaar having apparent activation energies (54 and 56 kJ mol<sup>-1</sup>) lower than those reported here. Recently, Gillooly et al. (2001) described universal temperature dependence, the concept that suggests that the temperature dependence of metabolic rates is nearly identical for all forms of life on Earth. The average  $E_a$  of Gillooly et al. (2001; 63 ± 14 kJ mol<sup>-1</sup>) is essentially the same as the average of values reported here (67 ± 15 kJ mol<sup>-1</sup>).

*Spatial differences in sediment reactivity*—Similar bottom-water temperatures throughout the estuary during each cruise means that measured values of  $E_{a-app}$  can also be used to evaluate spatial heterogeneity of sediment reactivity. The range in  $E_{a-app}$  from 0–1 cm is Sta. 3 < Sta. 2 < Sta. 4 < Sta. 1 (Table 5), which suggests that the greatest sediment reactivity is at Sta. 3 and the lowest reactivity (i.e., more

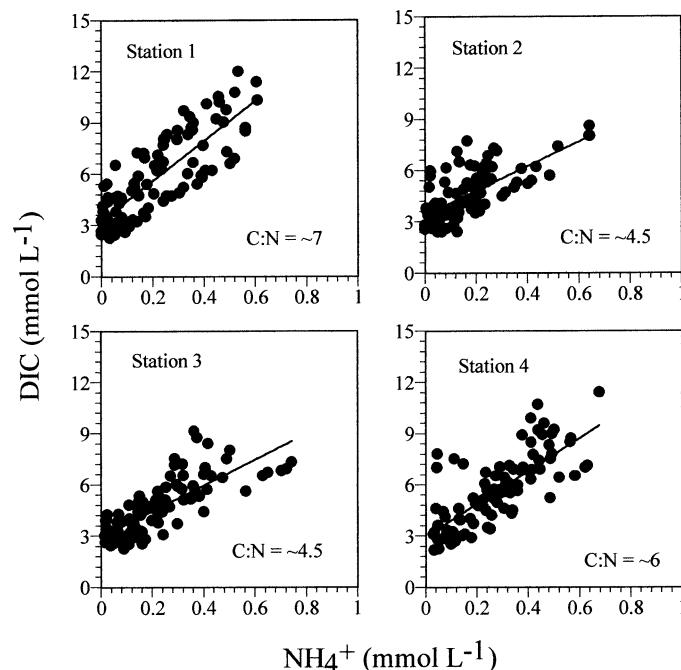


Fig. 7. C:N ratios in pore water at each station. DIC and  $\text{NH}_4^+$  concentrations represent the pooled data measured throughout the year at each station (excluding the surface 0.5-cm depth interval). Ratios are corrected for differential rates of diffusion of each ion.

refractory) is at Sta. 1. The percentage of organic matter, as measured by loss on ignition, showed no station-to-station differences (data not shown), with values consistently at ~10% by weight. However, we can evaluate the quality of organic material present in sediments at each station by pooling DIC and  $\text{NH}_4^+$  data measured in pore waters throughout the year (Fig. 7). Here we used pore-water data from deeper than 0.5 cm, the deepest point of  $\text{O}_2$  penetration during the study period (winter; data not shown), to ensure that C:N ratios are not biased by nitrification in the surface most sediments. C:N ratios (corrected for differential diffusion) of ~4.5 were measured at Sta. 2 and 3, which is consistent with the remineralization of recently formed organic matter and agrees with  $E_{a-app}$  predictions of greatest sediment reactivity at these sites. Similarly, C:N ratios of ~6 at Sta. 4 and ~7 at Sta. 1, although still indicative of reactive carbon, correlated with the  $E_{a-app}$  predictions of slightly lower sediment reactivity at these stations.

*Seasonal changes in sediment reactivity*—Averaged DIC production ( $\mu\text{mol cm}^3 \text{d}^{-1}$ ) in incubated sediments from Casco Bay showed strong seasonal variability, as illustrated in Fig. 8. Beginning in March (C5), DIC production increased more sharply in surface (0–1 cm) than in deeper (both 1–2 and 2–3 cm) sediments, peaking during the summer months. Differences in surface and deeper sediment DIC production rates again became minimal in winter (C12). Because there were no differences in temperature in at least the surface 5 cm of sediment during any cruise, this seasonal divergence in  $R$  is likely to have been caused by the deposition of more labile organic carbon to surface sediments relative to deeper

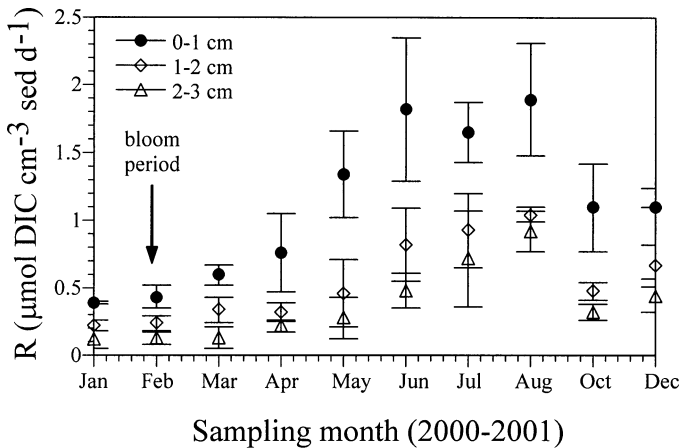


Fig. 8. DIC production rates ( $\mu\text{mol DIC cm}^{-3} \text{ sed d}^{-1}$ ) averaged ( $\pm$ SD) from the four study stations for the 0–1, 1–2, and 2–3 cm depth intervals of sediment throughout the year in Casco Bay. Rates in the 0–1 cm interval increased more rapidly after deposition of the spring phytoplankton bloom relative to sediments deeper in the deposit (1–2 and 2–3 cm).

in the deposit. Surface-water Chl *a* was significantly higher during the February cruise (C4;  $8.7 \pm 2.2 \mu\text{g L}^{-1}$ , Table 1) than during preceding and subsequent cruises, which likely reflects the beginning or end of the spring phytoplankton bloom that typically occurs during February (Teegarden et al. 2002). The deposition of bloom Chl *a* to underlying sediments should take  $<1\text{--}2$  d at these depths (Gerino et al. 1998), meaning that, by the March cruise (C5), bloom carbon should have long since been deposited to the SWI. It is interesting that, even after an entire month had passed after the deposition of the bloom to sediments, there appeared to be only a small reaction-rate divergence between surface and deeper DIC production rates by the March cruise (C5).

A period between bloom deposition and noticeable increases in diagenetic reaction rate is consistent with the knowledge that the complete oxidation of organic matter in sediments takes place through multiple steps, involves a number of bacterial species, and is dependent on temperature. In short, the complex organic polymers in phytoplankton (e.g., proteins and carbohydrates) must first be hydrolyzed to smaller-molecular-weight compounds (e.g., peptides, amino acids, and soluble saccharides) before their final conversion to carbon dioxide using the appropriate electron acceptor. The coupling of this multistep degradation process with the cold period associated with the “spring” bloom in temperate regions creates “lags” between deposition and reaction rate increases, as was apparently noted here. For example, Wu et al. (1997) reports a  $\sim 10$ -day lag before measurable increases in uptake rate of pore water acetate following the spring bloom in Long Island Sound, which occurred in late March when bottom water temperatures were  $0.1^\circ\text{C}$ . Schulz and Conrad (1995) report a similar lag in the coupled seasonality between acetate production and deposition of phytoplankton to lake sediments in a cold, deep lake. Green et al. (1998) reports a 14–21 day period before DIC production rate increased in Long Island Sound sediments following deposition of the spring phytoplankton

bloom (bottom water temperature  $0.1^\circ\text{C}$ ). In Casco Bay, cold bottom water temperatures during the period of bloom deposition (C4 =  $1.7^\circ\text{C}$ , C5 =  $0.4^\circ\text{C}$ ) would have slowed microbial activity, minimizing the stimulatory effects of labile carbon in surface sediments. By the April cruise (C6), bottom-water temperatures had increased to  $5.1^\circ\text{C}$  and reaction rates had accelerated enough to measure substantially higher DIC production in surface sediments using the incubation methods in this study.

*Solute transport across the SWI*—A quantitative understanding of solute flux across the SWI requires knowledge of both reaction rate and the mechanisms involved in the transport of solutes. Early diagenetic reactions and material exchange between sediments and water can be substantially increased by the activities of meio- and macrobenthos (Aller et al. 2001; Meile and Van Cappellan 2003). Extensive exchange between pore and overlying water can have dramatic effects on diagenetic reactions—for example, by not allowing reaction products to increase to levels that retard reaction rates and transporting  $\text{O}_2$  to regions of the deposit deeper than would occur otherwise (Aller et al. 2001). A similar exchange can result in the oxidation of reduced metabolites, leading to acid production, undersaturation with respect to carbonate minerals, and the dissolution of carbonates in nearshore regions (Green and Aller 1998).

In the present study, we used several methods to document rates of transport across the SWI, both spatially and temporally, throughout Casco Bay. The use of multiple methods is best when constraining rate measurements associated with early diagenetic processes. Constraints composed by the various assumptions and limitations associated with individual methods are minimized when those methods are compounded (Henrichs 1992; Gerino et al. 1998). Using the conservative tracer  $\text{Br}^-$ , we show an enhancement of fluid transport above that expected from molecular diffusion throughout most of the year in Casco Bay. Using fits from an explicit finite difference model (diffusion, no reaction, and finite overlying water volume), we documented a distinct seasonal pattern where, during spring, summer, and fall,  $\text{Br}^-$  loss from overlying water was faster than the loss by molecular diffusion. The station-averaged transport rate was  $\sim 2.4$  times ( $\pm 0.9$ ) faster than that of diffusive exchange during fall, spring, and summer (C2 and C6–C11), compared with 1.5 times ( $\pm 0.9$ ) faster during winter (C3–C5 and C12; Table 4, Fig. 6a).

Additional evidence of the seasonal dependence of biologically enhanced transport in Casco Bay comes from a direct comparison of the DIC production flux (sediment incubations) to the DIC gradient flux (Tables 2, 3). Figure 9 shows that DIC production flux estimates are consistently higher than those based on molecular diffusion and pore-water gradients, with production flux throughout the year  $\sim 2.6$  times higher than diffusive-based values. The largest seasonal discrepancy was seen during spring, summer, and fall cruises, when the production flux was  $\sim 2.8$  times that of gradient estimates and was consistent with the seasonal differences noted above using the  $\text{Br}^-$  tracer (Fig. 6a). In light of significant bio-irrigation in Casco Bay deposits, our use of a molecular-diffusion coefficient ( $D_s$ ) on pore-water

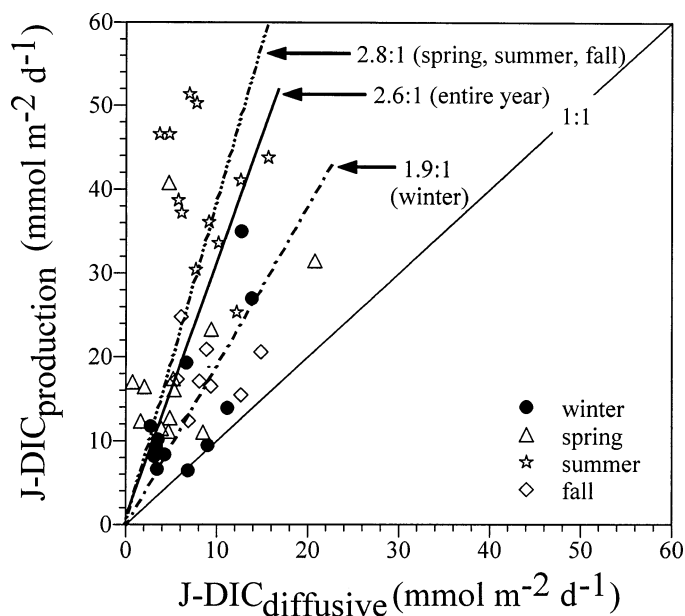


Fig. 9. Comparisons of DIC flux from sediment incubations ( $J\text{-DIC}_{\text{production}}$ ) to DIC flux from pore-water gradients ( $J\text{-DIC}_{\text{diffusive}}$ ) from each station during winter, spring, summer, and fall. Although no noticeable seasonal trend was seen, production flux estimates were consistently above those estimates that had been based on diffusion along pore-water DIC gradients. Incubation predicted that fluxes would be 2.8 times greater than diffusive estimates during spring, summer, and fall, 2.6 times greater than diffusive estimates during the entire year, and 1.9 times greater during winter.

gradients is one reason for low gradient flux relative to incubation-derived estimates. In addition, the high rates of bio-irrigation during spring, summer, and fall will further increase the discrepancies between flux methods, because irrigation during that period will lower DIC concentration gradients between pore and overlying water, thus lowering gradient flux estimates. A comparison of flux estimates during winter alone (Fig. 9) showed production flux  $\sim 1.9$  times higher than gradient estimates, which again is consistent with the lower transport coefficients documented during winter using  $\text{Br}^-$ -spiked cores.

A final estimate of the seasonal and spatial changes in transport can be made by model-fitting our DIC pore-water profiles. With the assumption of “local” steady state and our measured DIC production rates (Table 2), we can best fit measured pore-water DIC profiles (Fig. 4) using a one-dimensional, diffusion-reaction geometry according to Berner (1980):

$$\partial C/\partial t = 0 = D\partial^2 C/x^2 + R_o \exp^{-\alpha x} \quad (7a)$$

where  $C$  is the pore-water DIC concentration,  $x$  is the space coordinate, positive into sediment,  $D$  is the transport coefficient, either diffusive or biodiffusive ( $\text{cm}^2 \text{d}^{-1}$ ), and  $R_o$  is the reaction rate at the SWI and attenuating ( $\alpha$ ) with depth in the deposit. Physical advection was ignored because of low sedimentation rates in Casco Bay. “Local” steady state was assumed because the spatial scale of interest ( $<10$  cm) is small and the processes being measured are relatively fast compared with the time resolution of the study ( $\sim 1$ -month

sampling intervals). We assumed that the transport mechanism throughout Casco Bay (diffusive or biologically enhanced) could be described as mimicking random eddy diffusion caused by the high density and diversity of benthos known to exist there (Larsen et al. 1980; present study). As such, pore-water profiles and transport rate were estimated through curve fitting of measured DIC profiles using Eq. 7a, the reaction parameters generated from sediment incubations (Eq. 4, Table 2), and the boundary conditions

$$x = 0 \text{ cm}, \quad C = C_i \quad (7b)$$

$$x = L \text{ cm}, \quad \partial C/\partial x = B \text{ (basal gradient)} \quad (7c)$$

where  $C_i$  is the DIC concentration at the SWI (taken as the overlying water value). In this case, the basal gradient ( $B$ ) was taken as the concentration gradient from the deepest 2–4 data points or that region of each pore-water profile where DIC concentrations approach asymptotic values. Depth  $L$  was taken as the midpoint of depths used for estimates of the basal gradient,  $B$ .

Measured pore-water DIC concentrations and fits to pore-water DIC to model Eq. 7a–c are shown for Sta. 1–4 during winter, spring, summer, and fall in Fig. 4. There was good agreement between model and measured DIC in nearly all cases, which suggests that the methods used to calculate reaction parameters and assumptions regarding transport were valid. Although more complicated models exist for highly irrigated sediments (e.g., Boudreau 1997), good model fits suggest that there was no need to further complicate Eq. 7a–c with additional mathematical parameters (e.g., nonlocal exchange) and the various assumptions associated with them (i.e., Occam’s Razor). Likewise, there was good agreement between model estimates of transport using this model and the other methods described in the present study. The ratio of modeled estimates of transport to molecular diffusion coefficients,  $D_s$ , averaged for all stations, is shown in Fig. 6b. Seasonal patterns of transport control were similar to those documented using other methods, with transport accelerated predominantly during spring, summer, and fall cruises ( $\sim 3.5 \pm 1.6$  times diffusion; C2 and C6–C11) relative to winter ( $\sim 2.8 \pm 0.5$  times diffusion; C3–C5 and C12). Model estimates of transport were within range of the averaged enhanced diffusion using the  $\text{Br}^-$  tracer during, spring, summer, and fall (C2 and C6–C11; 2.4 times diffusion, Fig. 6a) and the comparison of production flux to diffusive flux estimates (2.8 times diffusion, Fig. 9).

*The role of benthos in material transport at the SWI—* The obvious explanation for the discrepancy between diffusive estimates of transport and measured transport using methods described above is that, during most of the year, transport is accelerated above rates governed by simple molecular diffusion by benthic organisms. Earlier work by Larson et al. (1980) showed that the benthic fauna in Casco Bay ( $>0.5$  mm) is rich in terms of diversity, density, and biomass. Larson et al. (1980) reported an average of 33 species per  $0.1 \text{ m}^2$  grab in each of 56 stations throughout the estuary, with average densities of  $\sim 9,000$  individuals  $\text{m}^{-2}$ . Relative numerical abundances of phylum encountered were annelids (42%), arthropods (26%), and mollusks (17%). Density val-

ues in particular were high relative to other temperate and boreal coastal deposits and help explain the rapid sediment irrigation documented in the present study. For comparison, Rowe et al. (1972) reported benthic densities of  $\sim 3,000$  individuals  $m^{-2}$  in the Mystic River Estuary. Maurer et al. (1978) gave densities of  $\sim 700$  individuals  $m^{-2}$  in Delaware Bay Estuary. Gerino et al. (1998) reported seasonal changes in macrobenthic density of 38 and 2,150  $m^{-2}$  during winter and summer, respectively, at a single station in central Long Island Sound. In the present study, we took grab samples for analysis of benthic fauna at each of our four stations during summer (C10) and found densities ( $>1.0$  mm) ranging from  $\sim 4,000$  individuals  $m^{-2}$  at Sta. 2 to  $\sim 7,000$  individuals  $m^{-2}$  at Sta. 4. Similar to the work of Larsen et al. (1980), numerical abundance was dominated by annelids, with the nephtyid polychaete *A. neotenus* and the spionid polychaete *P. steenstrupi* generally found in highest abundance. The polychaete *O. fusiformis* and the burrowing, deposit-feeding amphipod *C. bigelowi* were also numerically dominant.

Activities of these and other benthic organisms appear to increase throughout Casco Bay, beginning during spring and continuing through summer, radically enhancing exchange rates of solutes across the SWI. Seasonal changes in benthic activity have been reported elsewhere and appear to be coupled to increasing water temperature and the deposition of bloom-derived phytoplankton. For example, Martin and Sayles (1987) found bio-irrigation to only influence transport during summer, to minimally influence transport during fall, and found it not to be important during winter. Sun et al. (1991) noted an approximate threefold increase in particle mixing rates between February and April in Long Island Sound that were tightly coupled to deposition of the spring phytoplankton bloom and warming water temperatures. Gerino et al. (1998) saw a two–threefold increase in biodiffusive sediment mixing after deposition of the spring phytoplankton bloom in Long Island Sound. In the present study, the transport rate measured by all methods was substantially higher during spring, summer, and fall, with the initial shift toward biologically dominated exchange correlating with the spring phytoplankton bloom in Casco Bay estuary and the slow but progressive increase in bottom-water temperatures that were evident by the April cruise (C6).

Using a combination of sediment incubation experiments, analysis of pore-water gradients,  $Br^-$  tracer measurements, and a transport-reaction model, we showed that carbon decomposition and bio-irrigation were seasonally variable in Casco Bay estuary. Although some spatial heterogeneity existed among the four stations studied in both reaction rate and transport mode, the overall patterns were similar throughout the estuary. The highest rates of C-organic remineralization occurred during summer and correlated with the greatest enhancement of transport rate by the benthos. Transport by the benthos was adequately constrained by assuming a “quasi” or “enhanced” diffusion,  $D_{app}$ . The use of a  $D_{app}$  to describe transport appears to be reasonable in Casco Bay, given that competing infaunal, epifaunal, and molecular transport processes mimic random eddy diffusivity caused by the variety of transport processes generated by the very dense and diverse numbers of benthic species living there. The assumption that transport is driven solely by molecular

diffusion in Casco Bay will cause significant errors in calculations of flux between sediments and overlying water during most seasons.

## References

- ALLER, R. C. 1978. Experimental studies of changes produced by deposit feeders on pore water, sediment, and overlying water chemistry. *Am. J. Sci.* **278**: 1185–1234.
- , J. Y. ALLER, AND P. F. KEMP. 2001. Effects of particle and solute transport on rates and extent of remineralization in bioturbated sediments. *In* R. C. Aller, J. Y. Aller, and S. A. Woodin [eds.], *Organism-sediment interactions*. Univ. of South Carolina Press.
- BERNER, R. A. 1980. *Early diagenesis—a theoretical approach*. Princeton Univ. Press.
- BOUDREAU, B. P. 1986. Mathematics of tracer mixing in sediment. I—Spatially dependent, diffusive mixing. II: Non-local mixing and biological conveyor-belt phenomena. *Am. J. Sci.* **286**: 161–238.
- . 1997. Diagenetic models and their implementation: Modeling transport and reactions in aquatic sediments. Springer.
- CHANTON, J. P., C. S. MARTENS, AND M. B. GOLDBABER. 1987. Biogeochemical cycling in an organic-rich coastal marine basin. 7. Sulfur mass balance, oxygen uptake, and sulfide retention. *Geochim. Cosmochim. Acta* **51**: 1187–1199.
- CRILL, P. M., AND C. S. MARTENS. 1987. Biogeochemical cycling in an organic-rich marine basin. 6. Temporal and spatial variations in sulfate reduction rates. *Geochim. Cosmochim. Acta* **51**: 1175–1186.
- FISHER, J. B. 1982. Effects of macrobenthos on the chemical diagenesis of freshwater sediments, pp. 177–218. *In* P. L. McCall and M. J. S. Tevesz [eds.], *Animal-sediment relations: The biogenic alteration of sediments*. Plenum Press.
- FROELICH, P. N., AND OTHERS. 1979. Early oxidation of organic matter in pelagic sediments of the eastern equatorial Atlantic: Suboxic diagenesis. *Geochim. Cosmochim. Acta* **43**: 1075–1090.
- GERINO, M., R. C. ALLER, C. LEE, J. K. COCHRAN, J. Y. ALLER, M. A. GREEN, AND D. HIRSCHBERG. 1998. Comparison of different tracers and methods used to quantify bioturbation during a spring bloom:  $^{234}Th$ , luminophores, and chlorophyll-*a*. *Estuar. Coast. Shelf Sci.* **46**: 531–547.
- GILLOOLY, J. F., J. H. BROWN, G. B. WEST, V. M. SAVAGE, AND E. L. CHAMOV. 2001. Effects of size and temperature on metabolic rate. *Science* **293**: 2248–2251.
- GOLDBABER, M. B., R. C. ALLER, J. K. COCHRAN, J. K. ROSENFELD, C. S. MARTENS, AND R. A. BERNER. 1977. Sulphate reduction, diffusion and bioturbation in Long Island Sound sediments: Report of the FOAM group. *Am. J. Sci.* **277**: 193–237.
- GREEN, M. A., AND R. C. ALLER. 1998. Seasonal patterns of carbonate diagenesis in nearshore terrigenous muds: Relation to spring phytoplankton bloom and temperature. *J. Mar. Res.* **56**: 1097–1123.
- , AND ———. 2001. Early diagenesis of calcium carbonate in Long Island Sound sediments: Benthic fluxes of  $Ca^{2+}$  and minor elements during seasonal patterns of net dissolution. *J. Mar. Res.* **59**: 769–794.
- , ———, J. K. COCHRAN, C. LEE, AND J. Y. ALLER. 2002. Bioturbation in shelf/slope sediments off Cape Hatteras, North Carolina: The use of  $^{234}Th$ , Chl-*a*, and  $Br^-$  to evaluate rates of particle and solute transport. *Deep-Sea Res. II Top. Stud. Oceanogr.* **49**: 4627–4644.
- HALL, P. O. J., AND R. C. ALLER. 1992. Rapid, small-volume, flow

- injection analysis for CO<sub>2</sub> and NH<sub>4</sub><sup>+</sup> in marine and freshwaters. *Limnol. Oceanogr.* **37**: 1113–1119.
- HENRICH, S. M. 1992. Early diagenesis of organic matter in marine sediments: Progress and perplexity. *Mar. Chem.* **39**: 119–149.
- , AND J. W. FARRINGTON. 1987. Early diagenesis of amino acids and organic matter in two coastal marine sediments. *Geochim. Cosmochim. Acta* **51**: 1–15.
- JAHNKE, R. A. 2001. Constraining organic matter cycling with benthic fluxes, p. 302–319. *In* B. P. Boudreau and B. B. Jørgensen [eds.], *The benthic boundary layer*. Oxford Univ. Press.
- LARSEN, P. F., A. C. JOHNSON, AND L. F. DOGGETT. 1980. Environmental Benchmark studies in Casco Bay—Portland Harbor, Maine, April 1980. NOAA Technical Memorandum NMFS-F/NEC-19.
- LI, Y. H., AND S. GREGORY. 1974. Diffusion of ions in sea water and in deep-sea sediments. *Geochim. Cosmochim. Acta* **38**: 703–714.
- MACKIN, J. E., AND K. T. SWIDER. 1989. Organic matter decomposition pathways and oxygen consumption in coastal marine sediments. *J. Mar. Res.* **47**: 681–716.
- MARTENS, C. S., R. I. HADDAD, AND J. P. CHANTON. 1992. Organic matter accumulation, remineralization, and burial in an anoxic coastal sediment. *In* J. K. Whelan and J. W. Farrington [eds.], *Organic matter: Productivity, accumulation, and preservation in recent and ancient sediments*. Columbia Univ. Press.
- , AND J. V. KLUMP. 1984. Biogeochemical cycling in an organic-rich coastal marine basin. 4. An organic carbon budget for sediments dominated by sulfate reduction and methanogenesis. *Geochim. Cosmochim. Acta* **48**: 1987–2004.
- MARTIN, W. R., AND G. T. BANTA. 1992. The measurement of sediment irrigation rates: A comparison of the Br- tracer and <sup>222</sup>Rn/<sup>222</sup>Ra disequilibrium techniques. *J. Mar. Res.* **50**: 125–154.
- , AND F. L. SAYLES. 1987. Seasonal cycles of particle and solute transport processes in nearshore sediments: Rn-222/Ra-226 and Th-234/U-238 disequilibrium at a site in Buzzards Bay, MA. *Geochim. Cosmochim. Acta* **51**: 927–943.
- MAURER, D., L. WATLING, P. KINNER, W. LEATHEM, AND C. WETHE. 1978. Benthic invertebrates assemblages of Delaware Bay. *Mar. Biol.* **45**: 65–78.
- MCNICHOL, A. P., C. LEE, AND E. R. M. DRUFFEL. 1988. Carbon cycling in coastal sediments: 1. A quantitative estimate of the remineralization of organic carbon in the sediments of Buzzards Bay, MA. *Geochim. Cosmochim. Acta* **52**: 1531–1543.
- MEILE, C., AND P. VAN CAPPELLEN. 2003. Global estimates of enhanced solute transport in marine sediments. *Limnol. Oceanogr.* **48**: 777–786.
- MIDDELBURG, J. J., G. KLAVER, J. NIEUWENHUIZE, A. WIELEMAKER, W. D. HAAS, T. VLUG, AND J. VAN DER NAT. 1996. Organic matter mineralization in intertidal sediments along an estuarine gradient. *Mar. Ecol. Prog. Ser.* **132**: 157–168.
- PRESLEY, B. J. 1971. Techniques for analyzing interstitial water samples. Part I: Determination of selected minor and major inorganic constituents. Initial Rep. Deep-Sea Drilling Project **2**: 1749–1755.
- ROWE, G. T., P. T. POLLONI, AND J. I. ROWE. 1972. Benthic community parameters in the lower Mystic River. *Int. Rev. Ges. Hydrobiol.* **57**: 573–584.
- SCHULZ, S., AND R. CONRAD. 1995. Effect of algal deposition on acetate and methane concentrations in the profundal sediment of a deep lake (Lake Constance). *FEMS Microbiol. Ecol.* **10**: 251–260.
- SOLOZANO, L. 1969. Determination of ammonia in natural waters by the phenylhypochlorite method. *Limnol. Oceanogr.* **29**: 799–801.
- SUN, M. Y., R. C. ALLER, AND C. LEE. 1991. Early diagenesis of chlorophyll-*a* in Long Island Sound sediments: A measure of carbon flux and particle reworking. *J. Mar. Res.* **49**: 379–401.
- VAN DER BORGH, J. P., R. WOLLAST, AND G. BILLEN. 1977. Kinetic models of diagenesis in disturbed sediments. Part I. Mass transfer properties and silica diagenesis. *Limnol. Oceanogr.* **22**: 787–793.
- VOSJAN, J. H. 1974. Sulfate in water and sediment of the Dutch Wadden Sea. *Neth. J. Sea Res.* **8**: 208–213.
- WESTRICH, J. T., AND R. A. BERNER. 1988. The effect of temperature on rates of sulfate reduction in marine sediments. *Geomicrob. J.* **6**: 99–117.
- WU, H., M. A. GREEN, AND M. I. SCRANTON. 1997. Acetate cycling in the water column and surface sediment of Long Island Sound following a bloom. *Limnol. Oceanogr.* **42**: 705–713.

Received: 22 May 2003

Accepted: 30 September 2003

Amended: 21 October 2003